

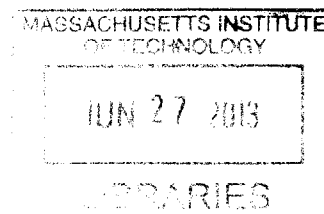
Electro-chemical Stimulation of Neuromuscular Systems Using Ion-Selective Membranes: Flexible Device Fabrication and Motor Unit Recruitment Order

by

Ragheb Mohamad Fawaz El Khaja

S.B. Mechanical Engineering
Massachusetts Institute of Technology, 2012

ARCHIVES



Submitted to the
Department of Biological Engineering
in Partial Fulfillment of the Requirements for the Degree of
Master of Engineering in Biomedical Engineering

at the

Massachusetts Institute of Technology

June 2013

© 2013 Massachusetts Institute of Technology. All rights reserved

Signature of Author
Department of Biological Engineering
May 22, 2013

Certified by
Jongyoon Han
Associate Professor of Biological Engineering
Thesis Supervisor

Accepted by
Forest White
Associate Professor of Biological Engineering
Chair of Graduate Program

Electro-chemical Stimulation of Neuromuscular Systems Using Ion-Selective Membranes: Flexible Device Fabrication and Motor Unit Recruitment Order

by

Ragheb Mohamad Fawaz El Khaja

Submitted to the Department of Biological Engineering
on May 22, 2013 in Partial Fulfillment of the
Requirements for the Degree of Master of Engineering in
Biomedical Engineering

ABSTRACT

Spinal Cord Injury (SCI) leads to paralysis, decrease in quality of life and high lifetime medical costs. Direct nerve Functional Electrical Stimulation (FES) induces muscles to contract by electrically stimulating nerves, which shows promise for clinical applications in restoring muscle function in SCI. However, Functional Electrical Stimulation is limited by the lack of graded response in muscle contraction and by high fatigability due to the reversal of recruitment order of motor units. Previous work showed that ion-selective membranes can be used to modulate Ca^{2+} ions *in situ*, decreasing the current threshold for nerve stimulation and eliciting a more graded muscle contraction response. This work developed polyimide-based cuff ion-selective electrodes to enable the future application of this technique *in vivo*. The developed electrodes were flexible, elastic and conductive. *In vitro* tests of the electrodes by stimulation of frog sciatic nerve reproduced the decrease in stimulation current threshold, which had been observed in planar glass-based electrodes, in the flexible polyimide-based electrodes. Additionally, cuffing the stimulated nerves with ion-selective electrodes was more effective at decreasing current threshold than planar stimulation. This work also analyzed data on twitch width, contraction time and relaxation time to infer effects of ion-selective electrodes on recruitment order. Stimulation with the ion-selective electrodes had higher twitch width, contraction time and relaxation time than traditional electrical stimulation at all force levels. The difference was particularly high at low force levels, indicating an effect of Calcium ion depletion on recruitment order.

Thesis Supervisor: Jongyoon Han
Title: Associate Professor

ACKNOWLEDGEMENTS

I am eternally grateful to my advisor Professor Jongyoon Han whose guidance and support made this work possible. Prof. Han, I appreciate your granting me freedom to pursue the topics I was interested in while giving me guidance in how to ask the right questions.

This work was supported in part by a fellowship from the Beth Israel Deaconess Medical Center and in collaboration with Dr. Samuel Lin MD, FACS. Conversations with Dr. Lin, and seminars hosted by him, were invaluable in motivating this research. I would like to acknowledge Dr. Ahmed Ibrahim, MD for providing surgical training and support.

This research was in many ways a continuation of previous work done by Prof. Yong-Ak Song during his time at MIT. Prof. Song's instruction and technical support were critical for this work. Additionally, some of the data presented here is further data analysis of experiments done by Prof. Song and Dr. Melik.

I would like to extend thanks to my lab mates: Aniruddh, Sha, Han Wei, Lidan, Rhokyun, Bumjoo for making the experience of working in the Micro/Nanofluidic BioMEMs lab an incredible one. I will miss you!

Last but not least, I thank my family, for always encouraging me to pursue my dreams. To my mother, Maha, for being my inspiration, supporting me every step of the way and loving me unconditionally. To my father, Fawaz, for sparking my interest in science, teaching me to question everything and sacrificing everything to afford me an education. To my sister, Aya, for pushing me forward and inspiring me to never give up. I love you all dearly.

*"If you can dream - and not make dreams your master;
If you can think – and not make thoughts your aim;"*
-Rudyard Kipling

Table of Contents

Abstract.....	3
Acknowledgements.....	5
Table of Contents.....	7
List of Figures.....	9
List of Tables	10
1. Introduction.....	11
2. Background.....	12
2.1. Spinal Cord Injury.....	12
2.2. Functional Electrical Stimulation.....	12
2.3. Clinical Applications of FES	12
2.4. Stimulation Configurations.....	13
2.5. Selective Direct Nerve Stimulation.....	13
2.5.1. Fiber Diameter Selectivity	13
2.5.2. Spatial Selectivity	15
2.6. Tissue and Electrode Damage.....	16
2.7. Flexible Cuff Electrodes	16
2.8. Ion-Selective Membranes	17
2.9. Role of Ca^{++} in Action Potential	17
2.10. Electrical Stimulation with Ca^{2+} ion Concentration Modulation	17
3. Methods.....	18
3.1. Flexible Polyimide Cuff Electrode Fabrication	18
3.1.1. Device/Mask Design.....	19
3.2. Polyimide Flexible Electrode Fabrication – Lessons Learned.....	20
3.2.1. Photoresist Deposition	20
3.2.2. Gold Adhesion to Polyimide.....	20
3.2.3. Etching Sacrificial Aluminum Layer	22
3.3. Calcium Ion Selective Membrane Deposition	23
3.4. Animal Preparation	23
3.5. Nerve Stimulation Experiments.....	24
4. Results and Discussion	25
4.1. Direct Nerve Stimulation with Flexible Polyimide Electrode	25
4.2. Motor Unit Recruitment Order	26

5. Conclusions.....	35
6. Appendix – Mask Design.....	36
Bibliography	37

List of Figures

Figure 1: Stained Cross-Section of a Single Fascicle in the Sciatic Nerve of a Cat.	15
Figure 2: Calcium Ionophore Type II (ETH 129).....	17
Figure 3: Schematic of Ion-Selective Tripolar Electrodes used by Song <i>et al.</i>	18
Figure 4: Flexible Polyimide Cuff Electrode Fabrication Process.....	18
Figure 5: Illustrations of Flexible Polyimide Electrode Design.....	19
Figure 6: Polyimide Electrodes with Poor Gold Adhesion.	21
Figure 7: Improved Gold Adhesion after Oxygen Plasma Treatment.	21
Figure 8: Improved Gold Adhesion with Chromium Tie-Coat.....	22
Figure 9: Polyimide Device Cuffed Around Frog Sciatic Nerve.	23
Figure 10: Experimental Setup for Nerve Stimulation	24
Figure 11: Proposed Design of Future Device.....	26
Figure 12: Sample Raw Data from Electrical Stimulation of Frog Sciatic Nerve.	27
Figure 13: Muscle Twitch Force Profiles with and without Ion-Selective Membrane.....	28
Figure 14: Definitions of Temporal Properties of Twitch Profile.....	29
Figure 15: Muscle Contraction Force vs. Stimulation Current.	30
Figure 16: Twitch Width vs. Stimulation Current..	30
Figure 17: Contraction Time vs. Stimulation Current.	31
Figure 18: Relaxation Time vs. Stimulation Current.	31
Figure 19: Twitch Width vs. Peak Force (% Max Peak Force)..	32
Figure 20: Contraction and Relaxation Time vs. Peak Force (%of Max Peak Force).	33
Figure 21: Photolithography Masks Design.....	36

List of Tables

Table 1: Properties of Different Muscle Unit Types.....	14
Table 2: Electric Current Threshold for Nerve Stimulation using Flexible Polyimide Electrodes.....	25

1. Introduction

Spinal cord injury has debilitating effects on a person's quality of life, often leading to paralysis, and is accompanied with high lifetime healthcare costs. Injuries to the spinal cord limit the conduction of signals between the central nervous system (CNS) and the periphery. Typically, the organs distal from the site of injury are physiologically intact but paralyzed due to lack of communication with the CNS. The intact nerves can be stimulated using electrical signals, leading to an action potential propagating down the nerve to the innervated muscle. The muscle contracts in response to this action potential producing a force. Functional Electrical Stimulation (FES) uses this phenomenon to restore neuromuscular function in patients with spinal cord injury.

While FES shows promise in clinical applications, it is limited by: high energy expenditure, limited spatial selectivity, and limited fiber type selectivity. According to the Henneman's size principle¹⁻³ of recruitment order, motor units are recruited in order of increasing size *in vivo*; small-diameter, slow twitch fibers are recruited first followed by large-diameter, fast twitch fibers. This recruitment order has the advantages of resistance to muscle fatigue and allowing the fine tuning of muscle force output. Electrical stimulation, however, recruits motor units in the opposite order, which imposes practical limitations on the clinical use of FES.

A novel technique for neuromuscular stimulation was recently developed by Song *et al.* based on *in situ* Ca^{2+} ion depletion using an ion selective membrane coupled with direct electrical stimulation of peripheral nerves⁴. This electrochemical technique was shown to decrease electric current threshold for muscle contraction by as much as 40% in *in vitro* experiments on frog sciatic nerves. Additionally, it was observed that the muscle contraction response to stimulating current is more gradual in the electrochemical technique than with traditional FES.

This work has two primary aims: 1) to fabricate and test a flexible polyimide cuff electrode with an ion-selective membrane in preparation for *in vivo* testing of this stimulation technique and 2) to quantitatively assess the effect of Ca^{2+} ion modulation on motor unit recruitment order.

In vivo testing of the electrochemical stimulation technique is critical for understanding the viability of the technology for applications in neuro-prosthetics. To enable *in vivo* testing, flexible polyimide-based cuff electrodes were fabricated by micro-fabrication and photolithography techniques and used to stimulate frog sciatic nerves *in vitro* with pulse trains.

The electrochemical stimulation technique is hypothesized to have a motor unit recruitment order more consistent with the Henneman's principle than that of standard Functional Electrical Stimulation. To test this hypothesis, frog sciatic nerve was stimulated with an electrical stimulation with and without Ca^{2+} ion modulation and the muscle contraction force temporal properties were analyzed.

2. Background

2.1. Spinal Cord Injury

Spinal cord injury (SCI) is a condition where nerves within the spinal canal are injured, usually caused by trauma to the vertebral column, which affects the brain's ability to send and receive signals from motor and sensory nerves below the level of injury. SCI has a high incidence rate with an estimated 10,000 new patients every year in the US, more than half of which are under 25⁵. The effects of SCI on patients' quality of life can be debilitating, ranging from pain to paraplegia to incontinence. Functional Electrical Stimulation is a promising alternative to current rehabilitation options⁵.

2.2. Functional Electrical Stimulation

When an electrical pulse is applied to a neuron, a localized electric field is generated which depolarizes the cell membrane. If this depolarization reaches a certain threshold, voltage gated Na^+ channels open, Na^+ ions rush into the intracellular space leading to the an action potential that propagates in both directions. The action potential that propagates away from the cell body is transmitted across a synapse either to a muscle (where it induces a contraction) or to another neuron⁶.

Paralyzed muscles can contract in response to the application of a current to the intact peripheral motor nerves. The contractions of different muscles could be electrically induced and coordinated in such a way as to provide function. This technique of restoring neuromuscular function is referred to as Functional Electrical Stimulation (FES). FES experiments started as far back as Galvani in 1780⁷. Soviet sports scientists used high intensity electrical stimulation to increase muscle force of elite athletes beginning in 1960s⁸.

2.3. Clinical Applications of FES

The application of FES requires the lower motor neurons to be excitable and the neuromuscular junction and muscle to be functional; thus it can be advantageous for patients of spinal cord injury (SCI), stroke, head injuries, cerebral palsy, and multiple sclerosis⁶.

FES has been demonstrated to have clinical applications in restoring function in a multitude of systems, including: Upper Extremities function, Lower Extremities function, Bladder and Bowel function, Respiratory function and Sexual function⁶.

Upper extremity neuro-prosthetics aim to restore use of hands in activities of daily living. Several systems have been developed that use implanted electrodes to achieve this goal⁹⁻¹².

One of the first uses for FES was to prevent foot drop (the foot dragging on the floor during gait), particularly for stroke patients. Implantable foot drop systems have been successfully demonstrated clinically^{13, 14}. Another objective of FES applications in lower extremities is to enable paraplegia patients to stand and transfer to another surface. As of 2005, no systems were FDA-approved for this application but one implantable system has reached multicenter clinical trial⁶.

Ambulation is considered the ultimate goal in lower extremity FES. Implanted systems for ambulation have been attempted with limited success. Rushton *et al.* attempted a 12-channel

system to activate L2-S2 motor roots which did not provide adequate selectivity¹⁵. Davis et al. used a cochlear implant-based technology, which allowed for standing and limited swing-through gait¹⁶. Another approach, developed in Cleveland, used stimulators/receivers implanted bilaterally, allowing the subject to stand and walk for 25 meters¹⁷.

Energy expenditure for walking by FES is fairly high; therefore, hybrid systems of electrical stimulation and external bracing are used to reduce energy requirements⁶. The bracing is used to support the weight of the patient, while FES is used to move the patient. However, these systems are difficult to wear and not aesthetically pleasing.

Up to Peckham 2005⁶, no system had been developed that allows ambulation without a walker or standing frame. This is due to stability, energy and muscle fatigue issues.

2.4. Stimulation Configurations

FES requires at least two electrodes for every nerve activated to achieve a current flow. Typically, function requires the coordination of the activation of several nerves. FES can be delivered through surface electrodes (commercially available) which are placed on the skin over the nerves. These electrodes, however, need to be repeatedly positioned to the right location, which can be non-trivial. Additionally, the surface electrodes may cause painful sensations due to nonspecific stimulation of pain receptors in the skin¹⁸. Furthermore, the several electrodes along with the leads, the stimulator and the control unit can attract unwanted attention and are not aesthetically pleasing. Therefore, it is desirable to design small, implantable systems that specifically stimulate neurons. Percutaneous systems present an intermediate between surface electrodes and implantable systems. In percutaneous systems, electrodes are implanted into the muscles to be activated and the leads are run out through the skin. These can activate deep muscles, produce repeatable contractions and do not cause painful nonspecific neuron activation⁶. Muscle-based stimulation has a high specificity but require more energy than nerve stimulation. Direct nerve stimulation provides more complete muscle recruitment and allows using one electrode to activate multiple muscles⁶. Therefore, this thesis concentrates on direct nerve stimulation.

Muscle contraction strength is influenced by the amplitude, frequency and duration of electrical pulses. Typically, the frequency of pulses is set constant and amplitude and duration of pulses are modulated to achieve the desired contraction strength.

2.5. Selective Direct Nerve Stimulation

An ideal nerve stimulation would require the ability to recruit motor units in the physiological recruitment order and to selectively activate different muscles that are innervated by the same nerve¹⁹. Current state-of-the-art FES techniques leave much to be desired in terms of stimulation specificity.

2.5.1. Fiber Diameter Selectivity

Fiber diameter selectivity is the ability to selectively stimulate nerve fibers based on size, to achieve physiological muscle unit recruitment order.

2.5.1.1. Henneman's Size Principle – Physiological Recruitment Order

Henneman's size principle of motor unit recruitment order dictates that motor units are generally recruited in order of smallest to largest as contraction increases in voluntary muscle contraction¹. Small motor units typically have low contraction force and slow contraction speed, but do not fatigue quickly (**Table 1**). Fast motor units typically have high contraction force and fast contraction speed but fatigue quickly. Therefore, this recruitment order has two major benefits: it allows the fine-tuning of force and decreases muscle fatigue.

2.5.1.2. FES Recruitment Order

When stimulated by FES, large diameter axons require less current to be activated than small axons. This is because the spacing between nodes of Ranvier is wider in larger axons, which leads to larger induced trans-membrane voltage changes⁶. Therefore, for increasing currents larger axons (and subsequently larger (type II) motor units) are activated before smaller axons (and motor units). This is a reversal of Henneman's size principle of recruitment order in voluntary muscle contraction. The larger motor units fatigue more quickly (**Table 1**), therefore, the reversal in recruitment order is detrimental for FES. Evidence of this reversal in recruitment order has been found in *in vitro* animal models^{20, 21}, and more recently, in *in vivo* human experiments²².

Table 1: Properties of Different Muscle Unit Types⁷.

Motor Unit Type	Axon Diameter	Muscle Fibers Area	Force Strength	Speed	Fatigue
Slow (S)/Type I	Small	Small	Low	Slow	Resistant
Fast Fatigue-Resistant (FR)/Type IIa	Large	Large	High	Fast	Resistant
Fast Fatigable (FF or FG) / Type IIb	Large	Large	High	Fast	Susceptible

Selective blocking of large diameter fibers allows fiber diameter selectivity in FES. By blocking large diameter fibers, physiological muscle recruitment order can be attained. Direct current can be used to block action potential conduction and it has been shown that blocking current threshold decreases with axon diameter^{21, 23}. However, direct current is undesirable for chronic applications since it causes neural damage (see **Section 2.6 Tissue and Electrode Damage**)²⁴⁻²⁶. Another drawback to DC block is anodic break: excitation when the hyper-polarization is ceased²⁷.

Additionally, High Frequency Alternating Current (HFAC) has been demonstrated to block action potential conduction²⁶. HFAC block has been used by Solomonow *et al.* to achieve normal recruitment order²⁸. HFAC block suffers from onset firing. Both DC block and HFAC block for fiber diameter selectivity require additional electrodes and stimulation channels, which

is undesirable²⁰. Other techniques involve more elaborate designing of stimulation pulse shapes. For example, quasi-trapezoid shaped long pulses were shown to selectively stimulate small diameter fibers²⁷. Single cathode electrode rectangular monophasic stimulation was also shown to selectively stimulate smaller fibers²⁰. Sub-threshold pre-pulse depolarization decreases excitability of large diameter axons to a higher extent than small diameter axons²⁷, therefore, it can be used to achieve fiber diameter selectivity in activation. All of these methods, however, require long stimulus pulse width which may lead to dangerous electrode corrosion.

In this work, we present a stimulation technique to achieve physiological recruitment order that does not require long stimulus pulse width or direct current block, hence avoids tissue and electrode damage associated with those techniques.

2.5.1.3. Fiber Diameter Spatial Distribution

The distribution of fiber diameters is an important factor in studies of fiber diameter selectivity of direct nerve stimulation. Studies have shown that in healthy adult human nerves, the distribution of axon diameters is bimodal²⁹. This is consistent with the characterization of motor units into Type I and Type II, with small and large axon diameters, respectively.

There is evidence that fiber diameter have uniform spatial distribution within fascicles. Thomas *et al.* found that the mean diameter of large diameter axons at the edge of a fascicle in human median nerve was not significantly different than that in the core of the fascicle³⁰. This uniform spatial distribution of fiber diameter implies that fiber diameter selectivity and spatial selectivity should be addressed as separate topics. This work focuses on fiber diameter selectivity due to its implications on motor unit recruitment order and muscle fatigue.

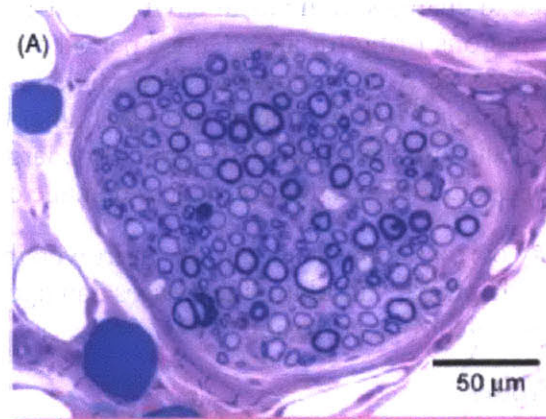


Figure 1: Stained Cross-Section of a Single Fascicle in the Sciatic Nerve of a Cat³¹.

2.5.2. Spatial Selectivity

Spatial Selectivity is the ability to selectively activate nerve fibers based on location in the nerve. Nerves commonly consist of multiple fascicles, small bundles of nerve fibers enclosed by the perineurium. Different fascicles in one nerve may innervate different muscles. Therefore, in order to restore muscle control by direct nerve stimulation FES, it is critical to achieve selective stimulation of different fascicles. Spatial selectivity can be achieved by placing the stimulating

electrodes in close proximity with the target since the threshold current is proportional to the square of the distance from electrode to target ²⁷.

Researchers at Case Western Reserve University developed a flat interface cuff electrode that changes the shape of the nerve to allow selective access to different fascicles for stimulation and recording ³². Yet, this technique has the possibility of deforming and damaging nerve fiber. Work by Tarler *et al.* demonstrated the use of ‘field steering’ of current to selectively stimulate different muscles from one nerve, by using a spiral cuff electrode with four radially placed mono-polar electrodes ³³. Yet, due to the generally conducting nature of the human tissue and fiber, it is unclear whether the electric current can be effectively ‘steered’ simply by the location of multiple stimulating electrodes. Older work by Durand *et al.* used a cuff electrode with radial projections that slowly penetrate into the interfascicular space outside of the perineurium, but within the epineurium of the nerve, placing the electrodes in closer vicinity to particular fascicles than others to allow selective stimulation of different nerve fascicles ¹⁹. Yet, the requirement of high current pulsing and other issues render the true spatial specificity in nerve activation challenging to achieve.

2.6. Tissue and Electrode Damage

Safety is a critical factor in designing an electrode or stimulation scheme for chronic applications. It is important to avoid damage to the tissue being stimulated and the electrode itself. Often there is a balance between efficacy (requiring enough charge per pulse to be effective) and safety (not exceeding tolerable charge per pulse).

Stimulation-induced tissue damage can be explained by two major mechanisms. Mass action theory attributes tissue damage to changes in the local environment due to induced hyperactivity from many neurons firing or neurons firing for an extended period of time ³⁴. Another proposed mechanism for tissue damage is toxicity of products of irreversible Faradaic reactions at the electrode during cathodic stimulation ³⁴. If this occurs at a rate higher than physiologically tolerable, tissue damage may occur. In current-driven stimulation, larger electrodes have fewer perturbations from their resting potential and, therefore, less damage due to Faradaic reactions.

Electrode damage is caused by corrosion of the electrode, an irreversible Faradaic reaction due to anodal driving of an electrode. Biphasic stimulation decreases damage due to electrochemical products at the cost of increased electrode corrosion ³⁴.

2.7. Flexible Cuff Electrodes

Direct nerve stimulation can be achieved *in vivo* by using cuff electrodes- electrodes that wrap around a nerve and allow stimulation of the nerve from all points circumferentially. Polyimide-based cuff electrodes have been used effectively for stimulation ³⁵ and recording ³⁶ in the peripheral nervous system. Polyimide electrodes are flexible, can be manufactured using micro fabrication techniques (allowing for small feature size) and have excellent mechanical stability, low biotoxicity and bio-reactivity ³⁷. These properties make polyimide an attractive substrate for neural implants.

Another promising technology for neural electrodes, being developed by Rogers *et al.*, uses ultrathin and flexible silicon nanomembrane transistors enabling high spatial resolution and flexibility, as well as CMOS-based advanced electronics embedded ³⁸.

2.8. Ion-Selective Membranes

Ionophores are molecules that bind to ions and form stable complexes. These molecules are naturally synthesized in the body and allow the transport of ions across lipid membranes. Ionophores are routinely used in ion-selective electrodes for sensing purposes. The ionophores are plasticized in polymeric membranes on electrodes, allowing the measurement of ion concentrations³⁹.

Calcium ionophore type II (ETH 129) is a molecule that binds to Ca^{2+} selectively in the sub-nanomolar range⁴⁰. The ionophore can be plasticized in PVC and printed on a negative electrode, leading to an *in situ* depletion of Ca^{2+} ions⁴.

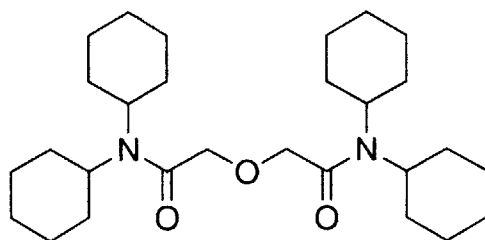


Figure 2: Calcium Ionophore Type II (ETH 129).

2.9. Role of Ca^{++} in Action Potential

It has been observed, in different animal models, that threshold current intensity of electrical stimulation decreases significantly when calcium concentration is lowered below a physiological level, while little change occurs when calcium concentration is varied above that level⁴¹. In the lower range of calcium concentration, frog sciatic nerves become more excitable, and below a certain threshold they may become spontaneously active⁴¹. When Calcium is removed from the nerve, spontaneous action potentials arise in the calcium deficient areas⁴¹. This is parallel to tetany observed when otherwise healthy individuals have low serum calcium.

2.10. Electrical Stimulation with Ca^{2+} ion Concentration Modulation

Recent work by Song *et al.* demonstrated a novel electro-chemical nerve stimulation technique that combines Ca^{2+} ion depletion and electrical current to reduce the electric threshold for stimulation⁴. The work used micro-fabricated planar gold electrodes and ion-selective membranes to electrically modulate ion-concentrations *in situ* along the nerve (Figure 3). It was found that this method reduced the stimulation current threshold by up to 40%. Interestingly, it was also observed that this electrochemical stimulation method induced a graded muscle contraction⁴. One possible explanation for this observation is that this technique restores (at least partially) physiological motor unit recruiting order. This work aims to investigate this hypothesis and shed light on the cause of this graded muscle contraction.

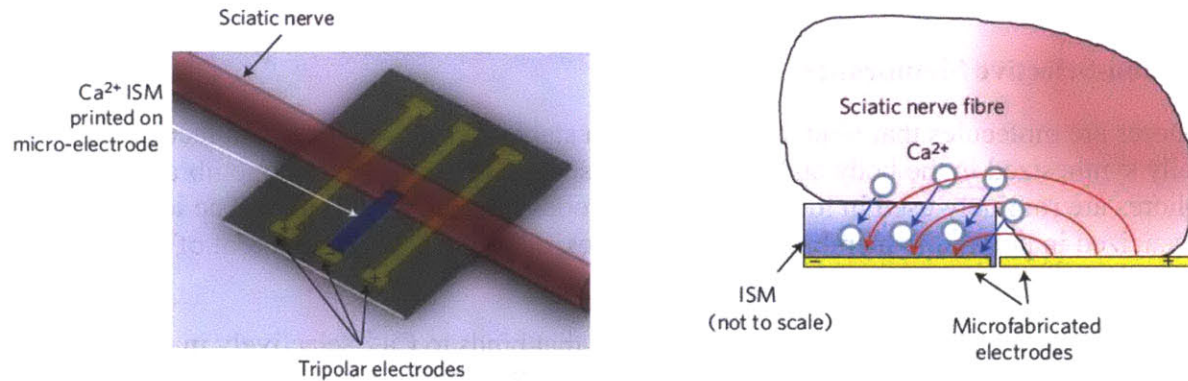


Figure 3: Schematic of Ion-Selective Tripolar Electrodes used by Song *et al.* ⁴.

3. Methods

3.1. Flexible Polyimide Cuff Electrode Fabrication

Flexible polyimide electrodes were fabricated with a gold lift-off technique using photodefinable polyimide. The devices consist of a base layer of polyimide, a layer of gold and a second layer of polyimide such that only contact areas in the gold are exposed. The fabrication process is illustrated in Figure 4.

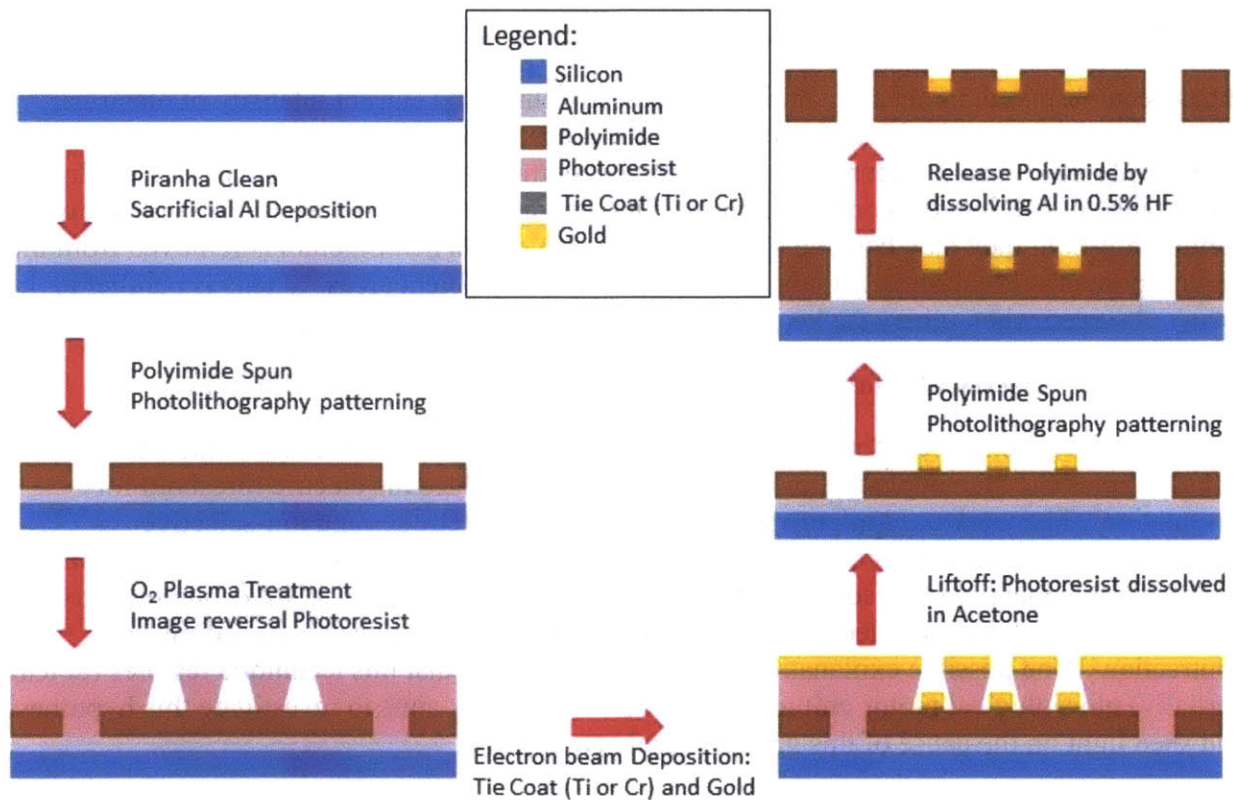


Figure 4: Flexible Polyimide Cuff Electrode Fabrication Process

A 6 inch Silicon wafer was cleaned by a standard Piranha clean, and then a 1 μm sacrificial layer of aluminum was deposited by electron beam lithography (Temescal Model VES2550).

Next, a first layer of polyimide was spun and patterned. The wafer underwent a 10 minute dehydration bake at 150 $^{\circ}\text{C}$, then photo-definable polyimide (Microsystems HD 4110) was applied by spin-coating for a target thickness of 15 μm (spread at 100rpm for 10s, then spun at 1500rpm for 30s). The polyimide was soft-baked at 110 $^{\circ}\text{C}$ for 4 minutes, then exposed to light for patterning using EVG Mask Aligner at 100J/cm² for 15s, then developed (HD Microsystems PA-401D for 80s) and rinsed with Propylene Glycol Monomethyl Ether Acetate. Subsequently, the polyimide was cured under N₂ at 360 $^{\circ}\text{C}$ for 1 hour.

To achieve gold patterning, image-reversal photoresist AZ 5214 was used in a liftoff process. The wafer was treated with oxygen plasma for 15minutes to improve adhesion. Then AZ 5214 was spin-coated for a target thickness of 1.5 μm (spread at 750rpm for 6s then spun at 1500rpm for 30s). Then the wafer was pre-baked at 95 $^{\circ}\text{C}$ for 30min, exposed using EVG Mask Aligner at 100J/cm² for 1.5s, post-exposure baked at 95 $^{\circ}\text{C}$ for 30min, then flood exposed at 100J/cm². Subsequently, the photoresist was developed in AZ 422 MIF for 4 min and rinsed in water. Electron beam deposition was used to deposit 10nm Titanium (or 25nm Chromium) tie-coat followed by 200nm Gold, followed by liftoff with acetone.

A second layer of polyimide was deposited and patterned in accordance with the above protocol such that the contact areas are exposed. Then the wafer was cut into individual devices using a die-saw. The sacrificial aluminum layer was dissolved to release polyimide from the wafer using a 0.5% HF solution for 4hrs, followed by 3 cycles of rinsing with water.

3.1.1. Device/Mask Design

The fabricated flexible electrodes need to be locked in place in the cylindrical (cuff) position. Several candidate locking mechanisms for the device were designed in AutoCAD. The design shown in Figure 5A was chose for simplicity and ease of application. The device is designed to be cuffed around the nerve followed by tying a small knot through each of two pairs of aligning holes stabilize the device.

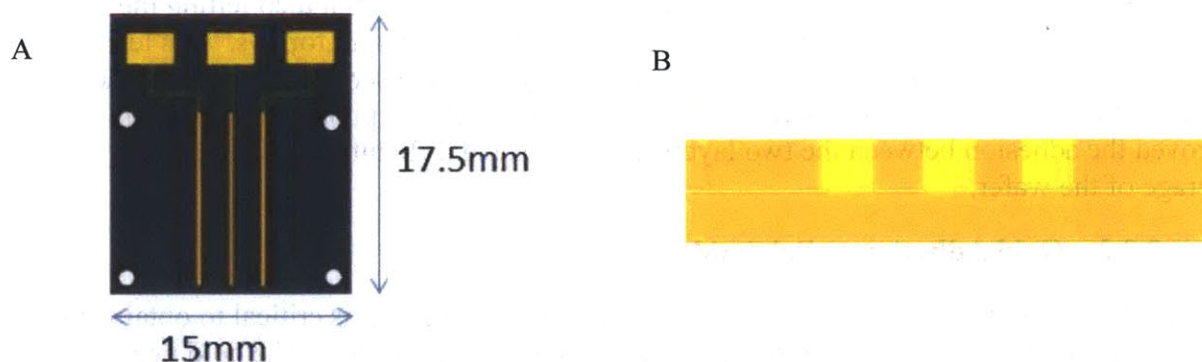


Figure 5: Illustrations of Flexible Polyimide Electrode Design A- Top View of Device (Black: Polyimide, Yellow: Exposed Gold, Green: Insulated Gold). B - Cross-Section of Device (Light Brown: Polyimide, Yellow: Gold). The device is composed of a base layer of polyimide, followed by a patterned layer of metallization, followed by a second layer of polyimide which is patterned so as to expose the wire contact pads and the electrodes.

Based on this device design, photolithography masks for 6 inch wafers were designed in AutoCAD so as to produce multiple devices, with different dimensions (distance between electrodes and length of electrodes) to allow experimenting with different devices. Three masks were designed: one for each of the two polyimide layers and one for patterning photoresist in the liftoff method for metallization. Alignment marks were included on the masks to enable the 2D alignment of patterns in the three layers. The masks used can be seen in the Appendix.

3.2. Polyimide Flexible Electrode Fabrication – Lessons Learned

Flexible polyimide-based electrodes were fabricated, as described in **Section 3.1**, with the goal of producing implantable cuff electrodes that can be used for direct nerve stimulation at the entire circumference of the nerve (as opposed to the stimulation at one point using flat glass electrodes ⁴). This section will describe the problems encountered and lessons learned during the fabrication iterations.

3.2.1. Photoresist Deposition

An image reversal photoresist (AZ 5214) was used in metal deposition after the first layer of polyimide was deposited, patterned and cured. The photoresist is used to pattern the deposited metal: photoresist is patterned so as to only cover regions that should not be metalized, then the entire wafer is metalized using e-beam deposition, then the underlying photoresist is dissolved resulting in the polyimide only being metallized in the desired regions.

Upon depositing the photoresist by spin-coating, we encountered difficulty getting full coverage of the wafer. In particular, there were regions radially outward from patterns on the underlying polyimide layer that were not covered by photoresist. The underlying polyimide had 1mm diameter holes in the pattern, creating an uneven surface for the spin-coating of the photo-resist. Upon spinning the wafer after dispensing the photoresist in the center, the photoresist moves radially outwards and is obstructed by the holes in the underlying polyimide leading to uneven coating of the wafer.

To reduce the effect of this problem, the entire surface of the wafer was coated with polyimide by dispensing the polyimide slowly over 12s as the wafer spins at 50rpm then letting the wafer rest for 5s before spreading at 750rpms for 6s then spinning at 3500rpm for 30s. This led to significantly improved coating of the wafer. Additionally, it was observed that treating the surface of the polyimide with oxygen plasma for 15minutes prior to photoresist deposition improved the adhesion between the two layers and eliminated difficulty in obtaining full coverage of the wafer.

3.2.2. Gold Adhesion to Polyimide

For successful fabrication and application of the flexible electrodes, it is critical to obtain strong adhesion between the gold electrodes and the underlying polyimide layer. The gold needs to remain adhered throughout the different steps in the fabrication process. Importantly, the adhesion needs to be strong enough to withstand bending of the device to form the cuff electrode.

The first iteration of devices was produced with a 10nm layer of titanium deposited between the 200nm gold layer and the underlying polyimide. These devices had poor adhesion and the gold peeled off during the etching of the sacrificial aluminum layer (Figure 6).

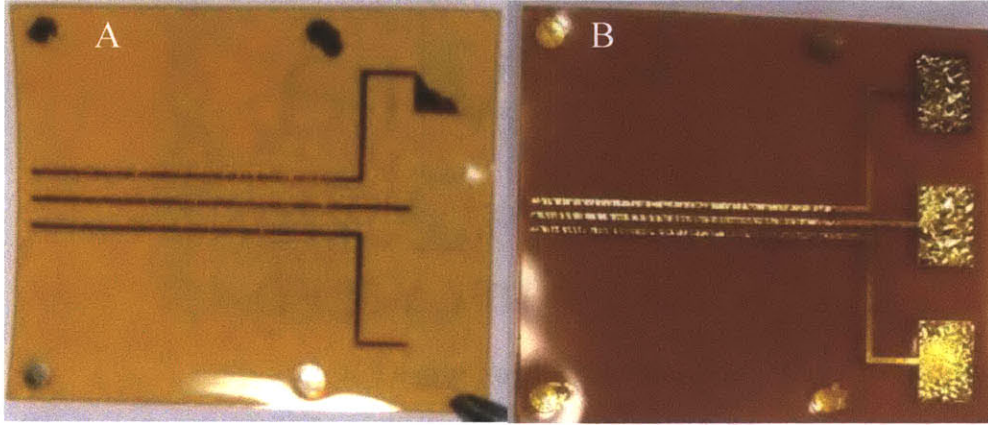


Figure 6: Polyimide Electrodes with Poor Gold Adhesion. A- Device with gold peeling at wire contact pads due to poor adhesion, B- Device with rough gold surface due to poor adhesion.

To improve adhesion, the surface of the underlying polyimide layer was treated by oxygen plasma (Branson/IPC low temperature plasma asher) for 15 minutes prior to the spin-coating of the photoresist layer and for 5 min prior to the e-beam gold deposition. This step resulted in improved adhesion such that the gold did not peel off during the fabrication process (Figure 7). This improved device allowed us to perform electrical stimulation experiments, but still had adhesion issues as evidenced by delamination of the gold and loss of conductivity during the stimulation experiments.

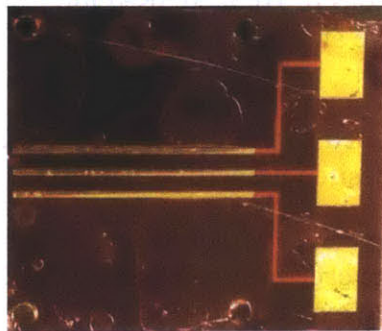


Figure 7: Improved Gold Adhesion after Oxygen Plasma Treatment.

To further improve gold adhesion, it was decided to use a layer of chromium as a tie-coat between the deposited gold and the underlying polyimide. This was based on research indicating that adding a chromium tie-coat improved the adhesion of copper to polyimide⁴² and fabrication protocols used by other labs^{43, 44} that used a thin Cr layer between Au and the polyimide to improve adhesion. This resulted in further improvement in Au adhesion, allowing repeated nerve stimulation with the device without loss of conductivity (Figure 8).

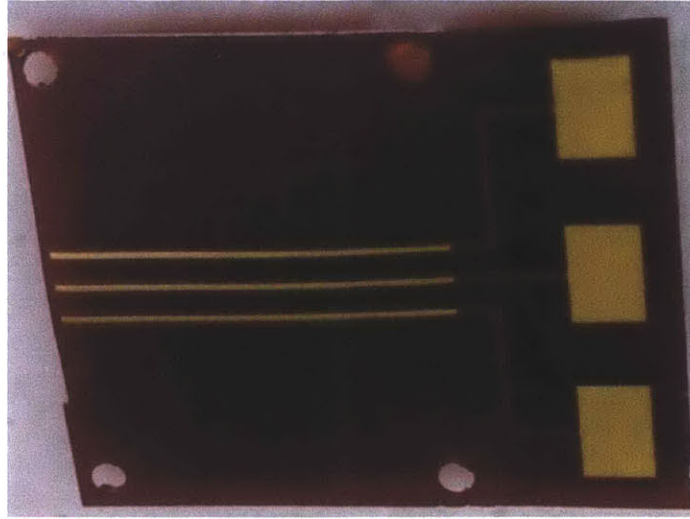


Figure 8: Improved Gold Adhesion with Chromium Tie-Coat

3.2.3. Etching Sacrificial Aluminum Layer

A sacrificial aluminum layer is used to separate the polyimide from the underlying silicon wafer. To remove the 1 μm thick Al layer, releasing the devices from the silicon wafer, a wet etch was used after cutting the 6 inch wafer into small individual devices. At first Aluminum Etchant type A (a mixture of phosphoric acid, nitric acid and acetic acid) was used at 60 $^{\circ}\text{C}$ for >24hrs. This treatment did not lead to any visible aluminum etching. The etchant has an etch rate of 24 nm/s at this temperature. Given that the etchant is only exposed to the aluminum on the edges of the device, it needs to etch through $\sim 10\text{mm}$ of material, which explains the ineffectiveness of this technique. Therefore, etching was attempted using 49% Hydrofluoric Acid (HF) which proved to be successful at dissolving aluminum but it also led to the delamination of the gold. Subsequently, different concentrations of HF were used for different time periods. It was found that 0.5% HF for 4 hours is effective at releasing the polyimide without peeling off the gold electrodes.

After incorporating the lessons learned in the fabrication process, a batch of polyimide-based gold electrodes that exhibited the desired properties of flexibility and conductivity.

The devices produced, seen in Figure 8, have conductive electrodes as evidenced by measurements of electric resistance; each electrode has $R \sim 50\Omega$ except for those with visually clear defects which were not used in experimentation. Additionally, the electrodes are not short circuited as evidenced by the high resistance between electrodes.

The fabricated devices were flexible and could be bent into radius of curvature $< 2\text{mm}$ without fracturing (Figure 9). The devices are fragile, however, and can tear easily especially if a small cut or kink is introduced accidentally.



Figure 9: Polyimide Device Cuffed Around Frog Sciatic Nerve.

3.3. Calcium Ion Selective Membrane Deposition

A Calcium-selective membrane was deposited on the microelectrodes using a microfluidic channel. The electrode was prepared for deposition by dehydration at 90°C on a hot plate for 24hr followed by silanization with N, N-dimethyltrimethylsilylamine (Fluka) for 60 min. A polydimethylsiloxane (PDMS) microchip with a single microfluidic channel was optically aligned using a stereomicroscope and sealed against the microelectrode. The calcium-selective material was produced using commercially available ion-selective cocktails from Sigma Aldrich, ETH129 (calcium ionophore II) for Ca^{2+} ion in Polyvinyl Chloride. Capillary force was used to fill the microchannel with the mixture (10-20 wt% Ca^{2+} ionophore in 35.8 mg PVC in 0.4 ml cyclohexanone), then the PDMS channel was removed and the electrodes were dried in a darkroom for 12h under ambient conditions.

3.4. Animal Preparation

In vitro testing of the technology was carried out on North American bullfrogs (*Rana Catesbeiana*), in accordance with a protocol approved by the Massachusetts Institute of Technology Committee on Animal Care. The frogs (average size 5 inch-6 inch) were purchased from Connecticut Valley Biological Supply Company and housed at the MIT Division of Comparative Medicine. The animals were moved from the animal facility to the lab then anesthetized with 2g/L MS222 (Ethyl 3-aminobenzoate methanesulfonic acid) for 30min-1hr, as confirmed by a toe pinch. The anesthetized frog was moved to the workspace and beheaded using scissors. Subsequently, the frog was double pithed using a pithing needle to obliterate the central nervous system. The frog was skinned using forceps. Then, the visceral area was dissected using forceps and dissecting scissors to access the sciatic nerves. The frog's upper torso and visceral organs were excised revealing the sciatic nerve - white cylinders running along each vertebral column. Blunt-tip forceps were used to secure the end of each sciatic nerve with a thread knot. The nerves were cleared from the surrounding tissue and passed through an incision in the frog's dorsal area and dissected through the hip and thigh down to the knee joint. A knot was tied around the Achilles tendon to allow attachment to the force transducer, then the gastrocnemius muscle was separated from the foot (leaving as much of the Achilles tendon as possible). Then muscle was separated from the leg by dissecting the inferior and superior portions of the knee joint while keeping the sciatic nerve attached to the gastrocnemius muscle.

3.5. Nerve Stimulation Experiments

The extracted sciatic nerves were stimulated using the tri-polar electrodes with an electric pulse train with increasing magnitude and the downstream muscle contraction force in the gastrocnemius muscle was measured. A function generator (Agilent 33220A) was used to produce a pulse train of frequency $f=1\text{Hz}$ and pulse width $t_p=1\text{ms}$ with increasing voltage outputs, which were transformed using a current isolator at 100 mA/V . The outputted current was used to stimulate the sciatic nerves through the tripolar electrodes connected, as shown in Figure 10, with a central negative electrode and two surrounding positive electrodes. The central electrode was coated with a micro-printed Ca^{2+} ion-selective membrane (ISM). The end of the gastrocnemius muscle innervated by the sciatic nerve was attached to a force transducer FT-302 (iWorx) with string. Simultaneous measurements of muscle contraction force and stimulating voltage were made using a data recorder (iWorx 214) at sampling frequency 100Hz . The data was analyzed using MATLAB and Labscribe2 software.

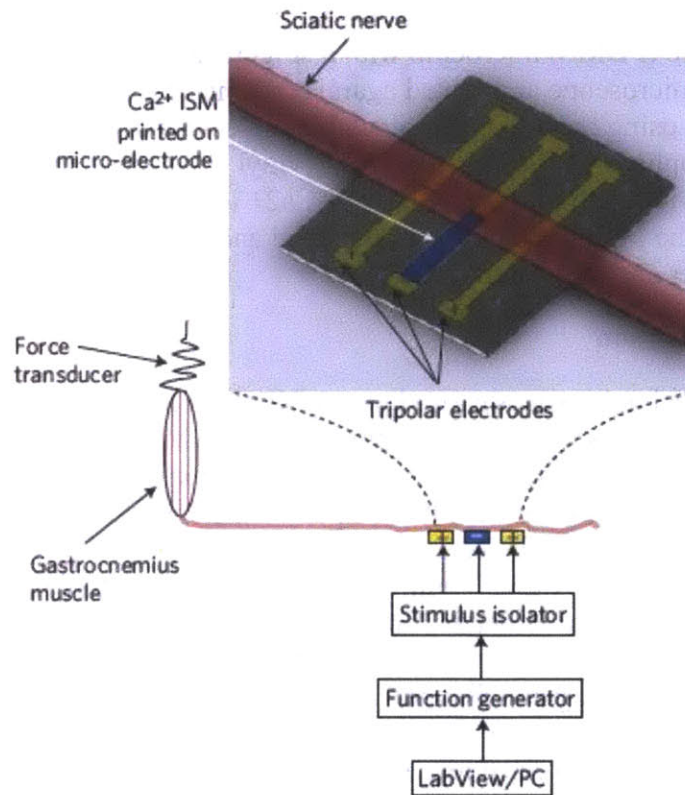


Figure 10: Experimental Setup for Nerve Stimulation ⁴.

4. Results and Discussion

4.1. Direct Nerve Stimulation with Flexible Polyimide Electrode

The micro-fabricated devices were tested *in vitro* by direct nerve stimulation of frog sciatic nerve while measuring muscle contraction force. The aim of this experiment is to assess the suitability of the flexible polyimide electrodes for electro-chemical stimulation of nerve. The technique for stimulation uses the same set-up as that used by Song *et al.*⁴. A sciatic nerve and the gastrocnemius muscle innervated by it were extracted from an American bullfrog (see Animal Preparation), and electric pulse trains ($f=1\text{Hz}$, width = 1ms) with increasing current amplitude were applied to the nerves through the devices in different device configurations: flat interface and wrapped around the nerve. Two devices were tested: with and without a Ca^{2+} ion -selective membrane surface-printed on the central electrode (cathode). The nerves were stimulated with current pulses with increasing amplitudes until muscle contractions were measured consistently at every pulse. The result of this experiment – the electric current threshold of nerve stimulation- is shown in Table 2.

Table 2: Electric Current Threshold for Nerve Stimulation using Flexible Polyimide Electrodes.

	Planar – with ISM	Cuffed - with ISM	Cuffed - no ISM
Nerve 1	10.6 μA	6.8 μA	N/A
Nerve 2	22.6 μA	19.1 μA	20.8 μA

As can be seen in Table 2, the flexible cuffed electrode allowed us to stimulate a frog sciatic nerve *in vitro*. The electrical current threshold for muscle contraction was decreased in both nerves when the flexible device was bent into the cuffed position. This result may indicate that electro-chemical stimulation using Ca^{2+} ion selective membrane is more effective when the electrode has full circumferential access to the nerve as opposed to only stimulating it at one point. Additionally, it can be seen in Nerve 2 that in the cuffed mode, the electrode with an ISM has a lower electric threshold than that with no ISM. This result is consistent with results obtained by previous work by Song *et al.* that showed that this technique decreases the electric threshold for stimulation of frog sciatic nerve with planar electrodes⁴. Further experiments are necessary to show the statistical significance of these two key results.

The mechanism used for securing the device in the cuffed position- tying a knot with a thin string to concentrically align two pairs of round holes in the polyimide- proved to be fragile and difficult to implement. The device often tore in the process of wrapping it around the nerve and securing it with the knots, making it difficult to carry out repeated *in vitro* experiments with the same device and limiting the ability to implant the device in future *in vivo* experiments. Due to the elasticity of the material, the device is under stress when bent into the cuffed shape. The device exhibits little plasticity and returns to original shape when released. The alignment holes focus the stress in a small area of the device leading to the tearing of the device.

This problem may be fixed in future iterations by rolling the devices into their final shape and tempering them (340 °C for 2h) to release stress in the bent position³⁵. By tempering the devices into shape, the neutral (unstressed) position would become the cuffed position. This would have

the dual advantage of decreasing difficulty in applying the device and decreasing chances of fracture of the device while in cuff position.

In addition to releasing stress by tempering the device, the locking mechanism should be redesigned to allow for easier manipulation of the device and flexibility in the diameter of the cuffed device. The design should enable the device to be locked and unlocked without any access issues or need for high precision in manipulation. Since nerves have varying diameters and it is important that the device is in contact with the nerves at all points circumferentially, there is a need for a device with adjustable diameter. This can be achieved by producing an elastic, flexible device tempered to a small neutral radius, such that it experiences light tension when applied around a larger nerve which insures full contact.

Several experiments were aborted due to tearing of the device at the site of wire applications. Additionally, for the purposes of implanting the device, it is preferable that the only electrically active (uninsulated) components are the electrodes in direct contact with the nerve. Therefore, it is proposed that the cuff electrode be connected to external wire contact pads through a long thin flexible extension as shown in Figure 11.

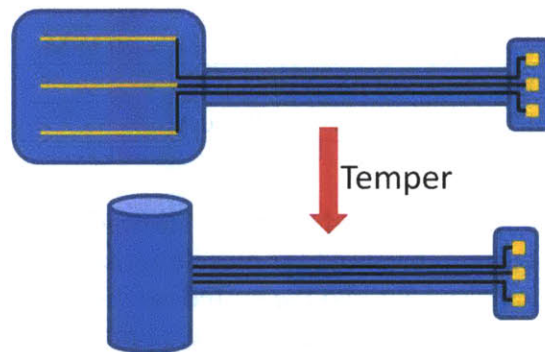


Figure 11: Proposed Design of Future Device. Blue underlying material illustrates polyimide, the gold lines show exposed gold electrodes and black lines indicate insulated gold leads.

This cuff electrode device needs further testing *in vitro* to confirm the results reported here: that increasing the surface contact area between the ion selective electrode and the nerve decreases the stimulation current threshold. Furthermore, the effect of further depletion of calcium ions through a sub-threshold ion depletion current should be assessed in the flexible device. Prior to clinical applications, this technology needs to be tested in *in vivo* animal models to confirm its biocompatibility, long-term stability and effectiveness when implanted.

4.2. Motor Unit Recruitment Order

It is hypothesized that this electrochemical stimulation technique may affect motor unit recruitment order, potentially reverting the recruitment order in Functional Electrical Stimulation back to the one observed physiologically as described by the Henneman's principle. To test this effect, data from *in vitro* direct nerve stimulation experiments using planar glass-based electrodes as described by Song *et al.* was analyzed. The time progression of muscle contraction force was analyzed to extract temporal properties of the muscle twitches. Previous work by Song *et al.* measured muscle contraction force with stimulation with a pulse train of increasing current amplitude. The data analysis done was focused on electric current threshold at which muscle

contraction is measured. In this section, we use data from experiments performed by Dr. Yong-Ak Song and Dr. Rohat Melik at Prof. Jongyoon Han's lab in addition to reproducing the data by new experiments. The data was analyzed to extract information about motor unit recruitment order through twitch width, contraction time and relaxation time.

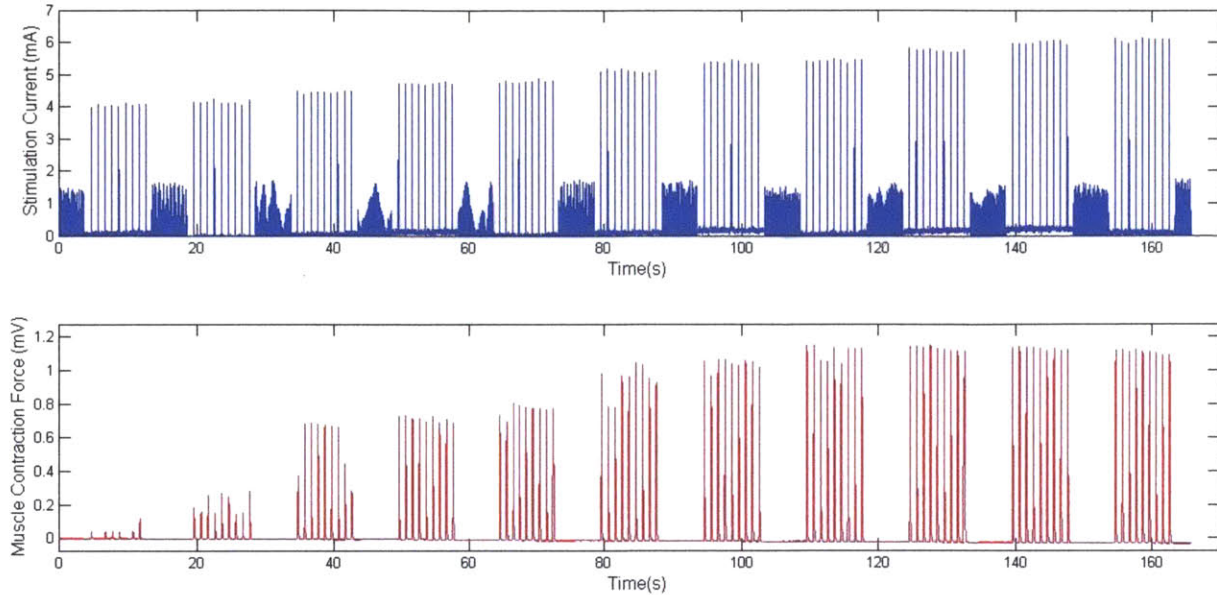


Figure 12: Sample Raw Data from Electrical Stimulation of Frog Sciatic Nerve. The sciatic nerve was stimulated by bare (no ISM) tripolar, flat electrodes and the muscle contraction force in the gastrocnemius was measured. The top figure (blue) shows the stimulation current applied to the nerve through the electrode. The bottom figure (red) shows the measured muscle contraction force.

A typical raw experimental result is shown in Figure 12. An input pulse train with gradual increase in pulse height (sets of 9 pulses of constant pulse height, $f=1$ Hz $t_p=1$ msec) leads to muscle twitches that start at a certain input threshold and increase in amplitude with increasing pulse height reaching a plateau (maximal contraction force). This result is consistent with expectations: as input current increases, the nerve fibers are recruited in order of increasing stimulation threshold until all of the nerve fibers are recruited.

Song *et al.* established that using a Ca^{2+} ion selective membrane decreased stimulation threshold by up to 40% compared to electrical-only stimulation⁴. By performing several experiments with the same setup as Song *et al.*, the results were replicated with average decrease in stimulation threshold of 15%.

To determine if the type of motor units recruited (fast vs. slow twitch) and the order of motor unit recruitment are affected by Ca^{2+} depletion by the ISM, the twitch profiles were analyzed. A twitch profile is a plot of muscle contraction force as a function of time for a single muscle twitch after stimulation with one electric pulse (zooming in on one peak in Figure 12). Each pulse train used produced 9 pulses (and subsequent twitch profiles) at every current level. Representative examples of typical single twitch profiles recorded in the cases of electric only stimulation (no ISM, control) and stimulation with an ion-selective electrode are shown in Figure

13. The twitches displayed were chosen to have an equal force amplitude (<5% difference) to allow comparison of temporal progression of force. It is observed that the electrochemical technique has a longer twitch time than the control. Additionally, it is observed that the time to peak (contraction time) is larger in the electrochemical technique than the control.

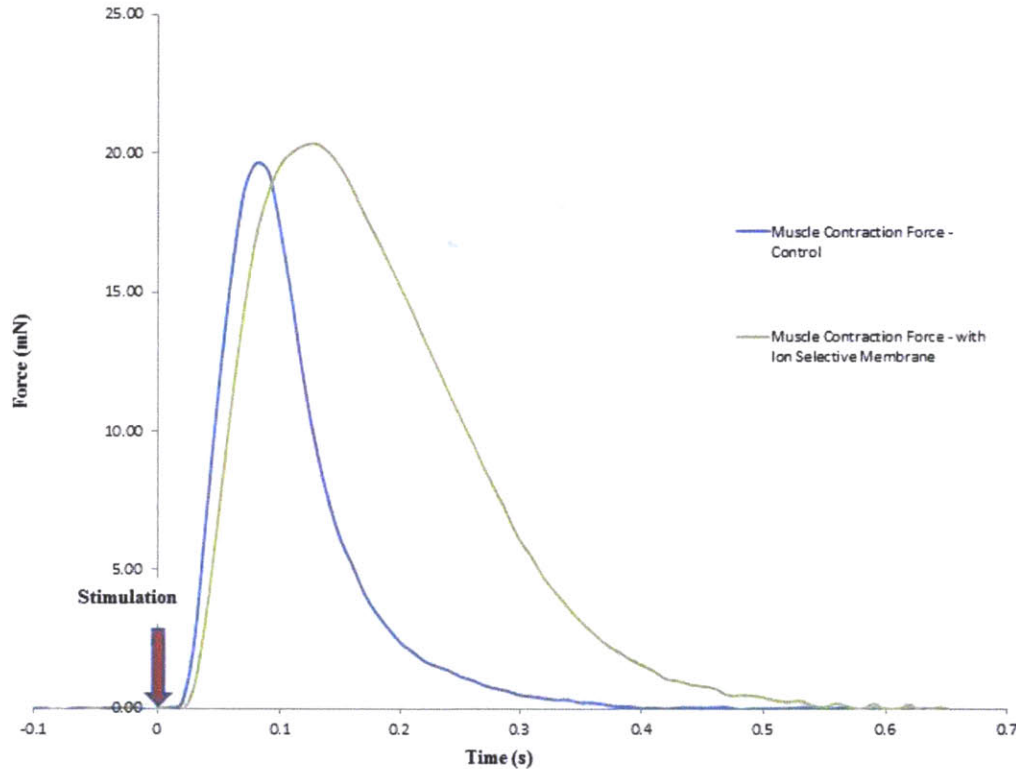


Figure 13: Muscle Twitch Force Profiles with and without Ion-Selective Membrane. Plot of muscle contraction force (mN) as a function of time in two muscle twitches induced by electrical stimulation: control with no ion selective membrane, shown in green, and the electro-chemical technique with Calcium ion selective membrane, shown in blue. The muscle twitches chosen had equal peaks.

Muscle contraction twitch force profiles data were analyzed using MATLAB to extract: twitch width, contraction time, relaxation time and latency time (Figure 14). Definitions of these parameters that were used by Fang *et al.* and Llewellyn *et al.* were adopted by this work^{20, 45}. Latency time is defined as the time from electrical stimulation until the muscle force reaches 10% of peak. Twitch width is the duration of the muscle twitch, defined as the time during which the muscle contraction force is greater than 10% of peak. Twitch width can be further broken down to contraction time and relaxation time. Contraction time is defined as the time from 10% to time of peak. Relaxation time is defined as the time for force decay from peak to 10%.

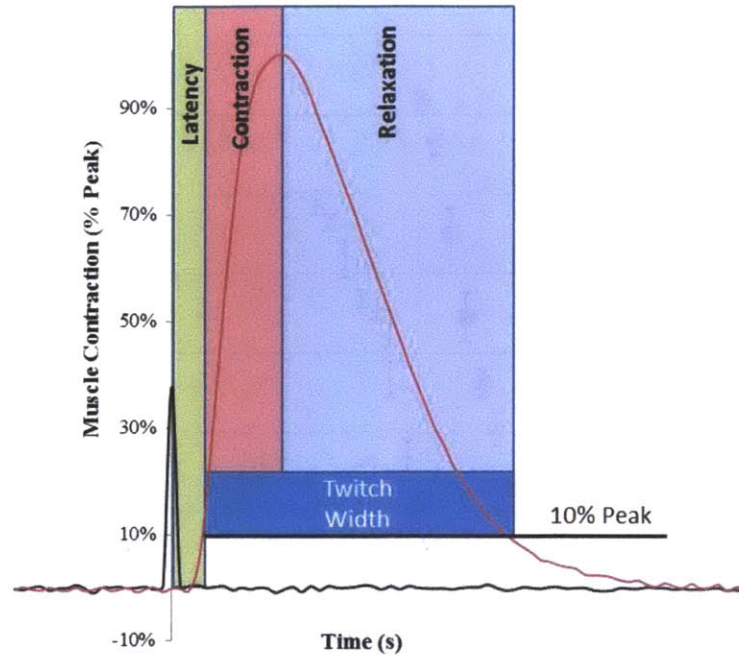


Figure 14: Definitions of Temporal Properties of Twitch Profile

Representative sample results from nerve stimulation of a sciatic nerve using a planar electrode with and without an ion-selective membrane as described in Methods (**Section 3.5**), are shown in Figures 15, 16, 17, 18. These are results from one pulse train for each type of stimulation, applied on a single sciatic nerve. Each data point represents the average of 9 stimulations at a particular current amplitude. The pulse train used consists of several sets of 9 stimulations of equal amplitude, at frequency 1 Hz. Stimulation starts at amplitude below threshold and each subsequent set has an amplitude $0.2\mu\text{A}$ higher until maximum contraction force is reached. Latency time data could not be extracted precisely because the time ($\sim 30\text{msec}$) was too low compared to the sampling frequency (100Hz). Figure 15 shows the dependence of muscle contraction force on stimulating current. Figure 16 allows the comparison of twitch width when the nerve is stimulated with ISM to a bare electrode control. Figures 17 and 18 breakdown the twitch width to contraction time and relaxation time to distinguish the ISM's effect on each.

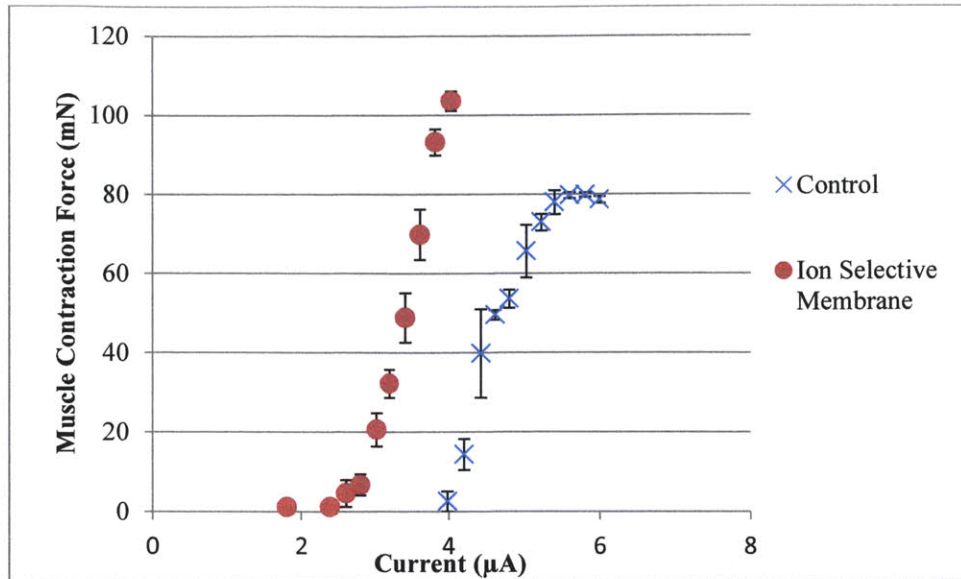


Figure 15: Muscle Contraction Force vs. Stimulation Current. Sciatic nerve was stimulated with a pulse train through an electrode with ISM (red dots) or without ISM (blue crosses). Each point is the average of 9 pulses; the error bars represent standard deviation.

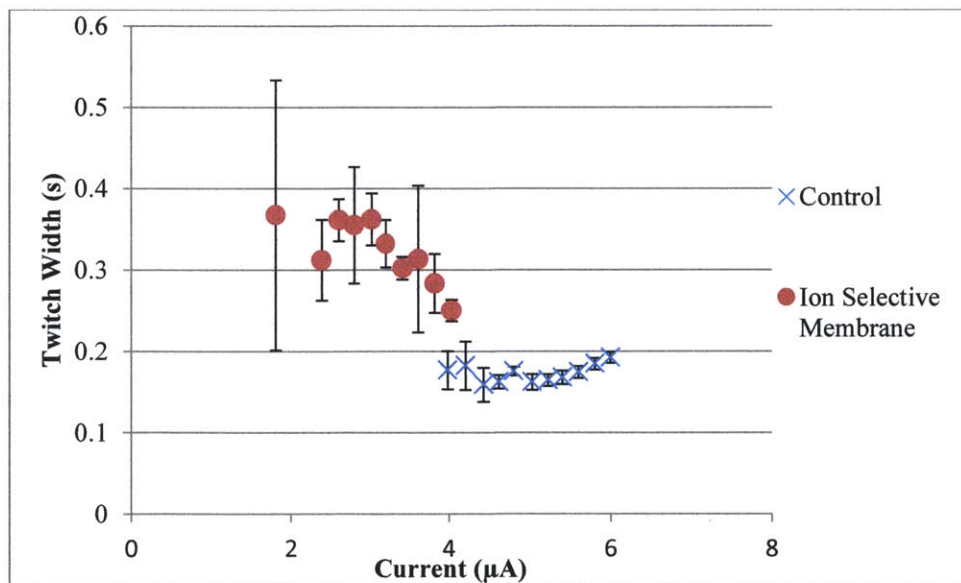


Figure 16: Twitch Width vs. Stimulation Current. Sciatic nerve was stimulated with a pulse train through an electrode with ISM (red dots) or without ISM (blue crosses). Each point is the average of 9 pulses; the error bars represent standard deviation.

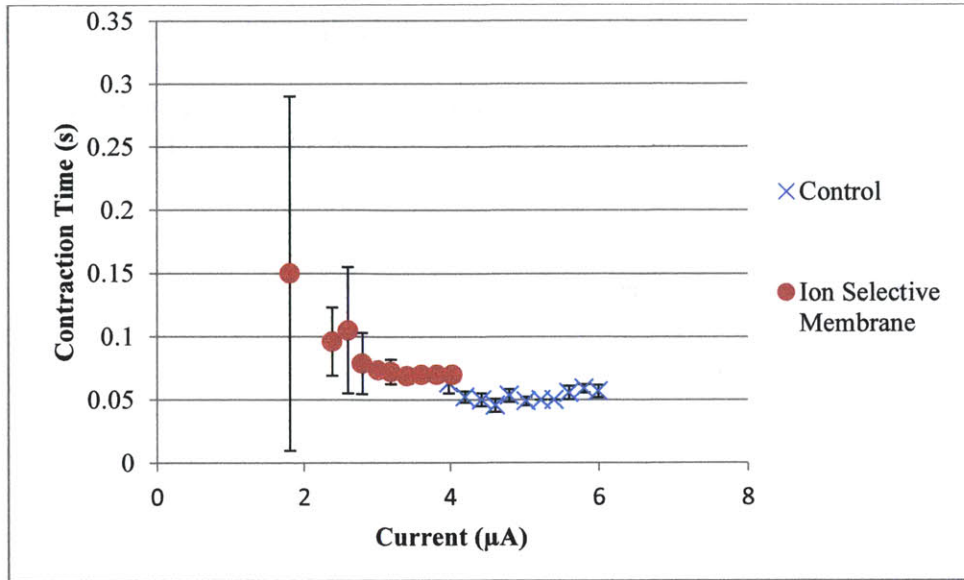


Figure 17: Contraction Time vs. Stimulation Current. Sciatic nerve was stimulated with a pulse train through an electrode with ISM (red dots) or without ISM (blue crosses). Each point is the average of 9 pulses; the error bars represent standard deviation.

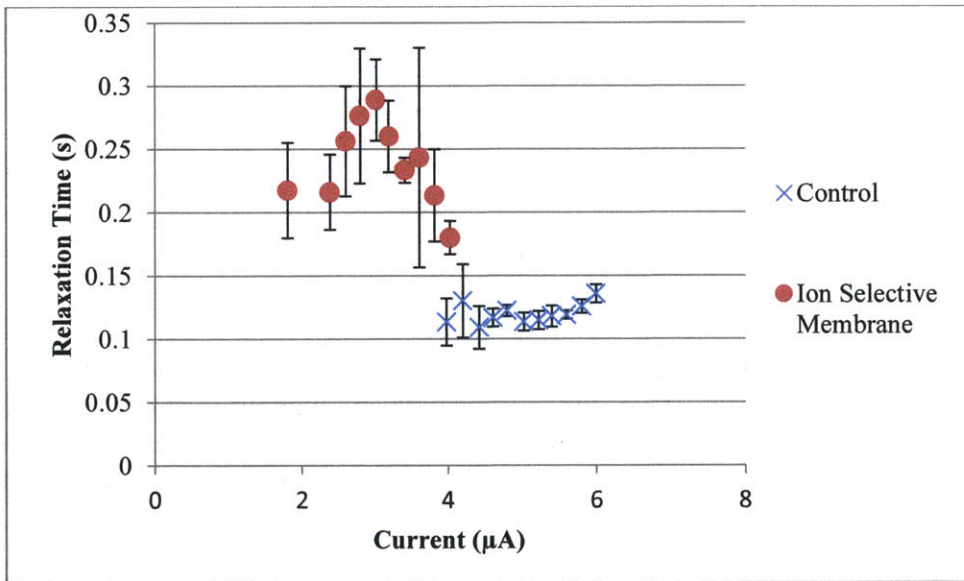


Figure 18: Relaxation Time vs. Stimulation Current. Sciatic nerve was stimulated with a pulse train through an electrode with ISM (red dots) or without ISM (blue crosses). Each point is the average of 9 pulses; the error bars represent standard deviation.

It can be observed from Figure 16 that muscle twitches from electric stimulation with Ca^{2+} ISM has higher twitch width than muscle twitches from electric stimulation without ISM. Figures 17 and 18 indicate that both contraction time and relaxation time contribute to this difference.

Due to differences in the threshold current of stimulation between the two techniques, it might be more appropriate to analyze the temporal properties of muscle twitches as a function of peak

force rather than as a function of stimulation current. This allows the aggregation of data from multiple stimulation pulse trains. Data on twitch width, contraction time and relaxation time from stimulating a nerve with 3 separate pulse trains for each stimulation method (ISM and control) were aggregated, sorted into by peak force amplitude (as a percentage of maximum measured peak force) and plotted in Figures 19 and 20.

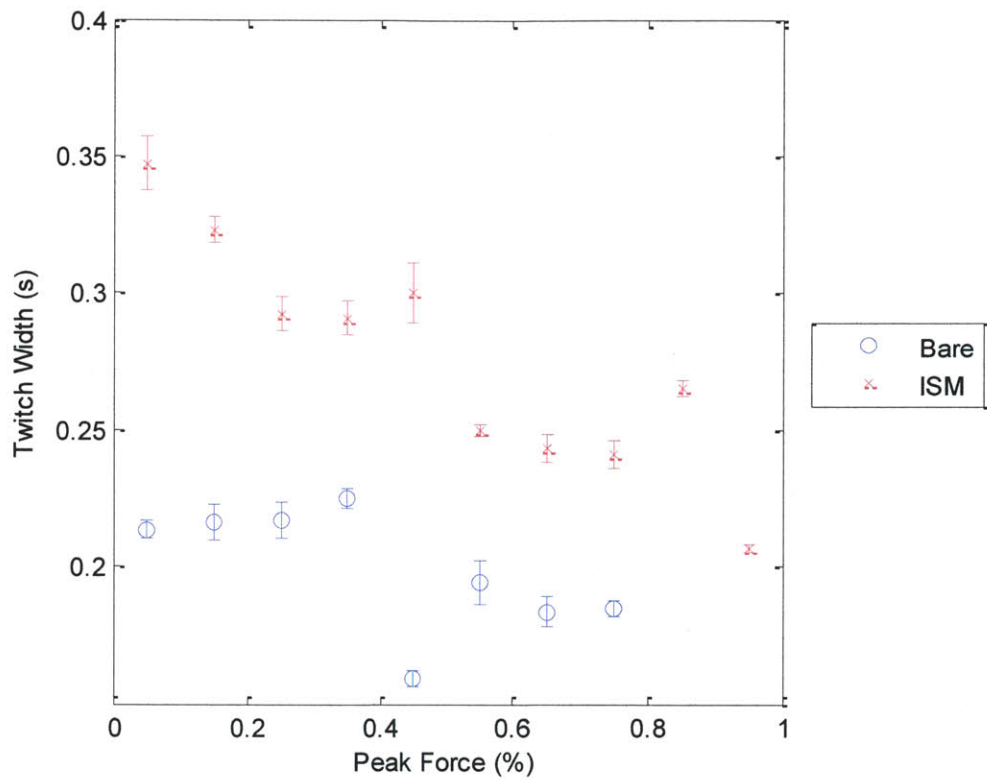


Figure 19: Twitch Width vs. Peak Force (% Max Peak Force). Muscle contraction twitch width measured from pulse train nerve stimulations with and without ISM plotted against peak force. The data is the aggregate of 3 separate stimulation pulse trains for each of the control and the ISM. The Control is shown as blue circles while the ISM is shown as red crosses. The error bars shown are standard error of mean.

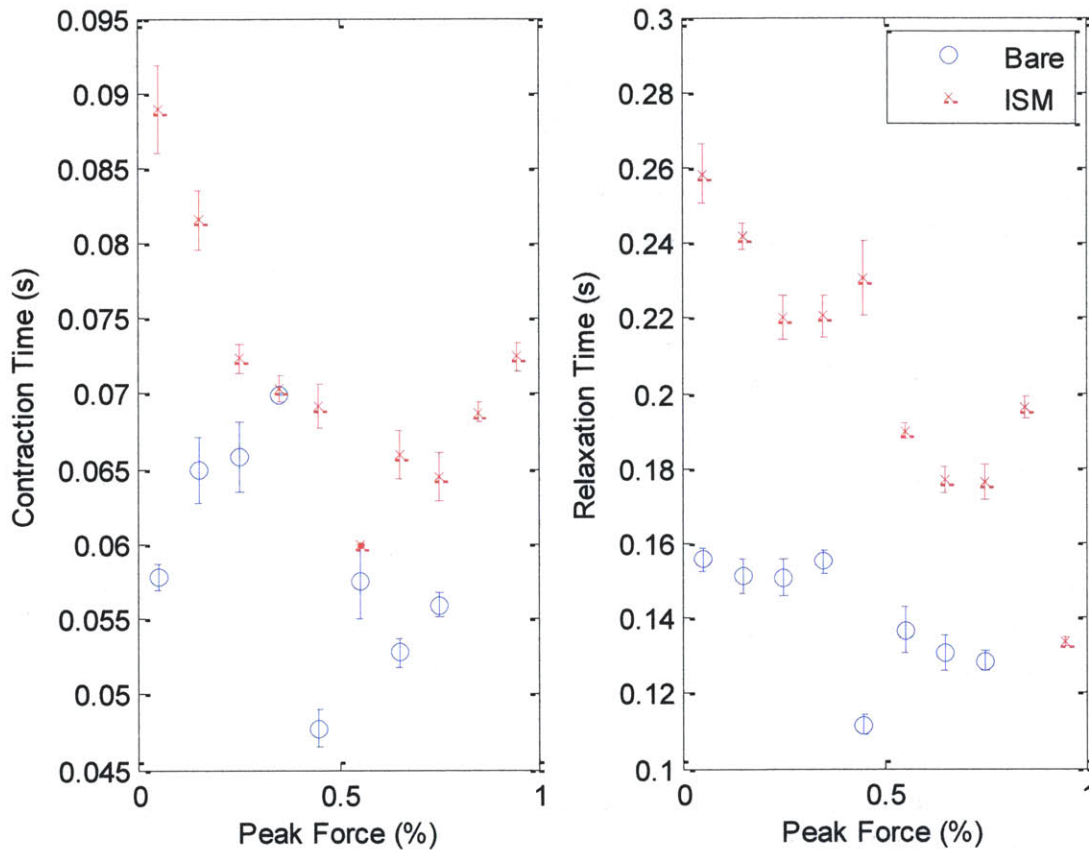


Figure 20: Contraction and Relaxation Time vs. Peak Force (% of Max Peak Force). Muscle contraction and relaxation time measured from pulse train nerve stimulations with and without ISM plotted against peak force. The data is the aggregate of 3 separate stimulation pulse trains for each of the control and the ISM. The Control is shown as blue circles while the ISM is shown as red crosses. The error bars shown are standard error of mean.

It can be observed from Figure 19 that stimulation using the ion-selective membrane results in a higher twitch width (at all levels of force) than stimulation with bare electrodes. It can also be observed that the twitch width in the ISM case is decreasing with increasing force. In Figure 20, it is observed that contraction time and relaxation time follow the same trend: they are both higher in ISM than in bare electrodes, particularly at low forces. This result is consistent with the hypothesis that stimulation with ISM preferentially stimulates slow twitch fibers at low force.

Slow twitch motor units are typically innervated by small diameter axons, which have a higher surface area to volume ratio than large diameter axons innervating fast twitch motor units. Assuming that the surface density of calcium channels is not dependent on axon diameter, a change in extracellular concentration of Ca^{2+} will have a greater effect on small diameter axons due to their higher surface area to volume ratio. This may explain the finding that coupling electrical stimulations to *in situ* Ca^{2+} depletion leads to an increase in recruitment of slow twitch fibers, particularly at low electrical stimulation.

On the individual motor unit level, fast twitch motor units have a significantly lower twitch width, contraction time and relaxation time than slow twitch motor units. In the medial gastrocnemius of cats, early work by Henneman found that the mean contraction time of fast twitch motor units is 80.4msec while that of slow twitch motor units is 34.6msec³. In large animals, it is possible to isolate individual motor units and identify their type (fast vs. slow) and then determine recruitment order in pairwise stimulation experiments. This is not possible in the small animals that were used in this work (bull frog), therefore, the data presented is from measurements of whole muscle contraction (not individual motor units).

When a nerve is stimulated (electrically or voluntarily), multiple motor units are recruited and the compound muscle contraction observed is the sum of the effects of the contraction of all of these individual motor units. It is argued that the compound muscle contraction's properties (including twitch width, contraction time and relaxation time) are affected by the properties of the recruited motor units. A muscle contraction with primarily slow twitch fibers is expected to have slower twitch than a muscle contraction with primarily fast twitch fibers. This argument was made implicitly by work done on optical nerve stimulation by Llewellyn *et al.*, which used comparison of compound muscle contraction properties to infer recruitment order⁴⁵. Furthermore, Fang *et al.* used data on twitch width from whole muscle contraction in concluding that quasi-trapezoidal pulses can be used to restore recruitment order²⁰. Fang *et al.* argued that using twitch width to determine recruitment order is more appropriate than using contraction time because contraction time can be highly biased by the effect of a few fast twitch contractions.

An alternative interpretation for the increase in twitch width in this stimulation setup is that different motor units are contracting at different points in time, leading to a longer twitch than if the motor units had all contracted at the same time. Given that the stimulation is occurring at the site of the nerve, there are two possible causes of such a delay: differences in conduction velocity and difference in lag from stimulation to initiation of action potential. If the recruitment order is indeed affected by the ISM, a wider range of conduction velocities would be observed, leading to a wider range of latency times and overestimation of the results. The latency time in these experiments was typically on the order of 30ms while the change in twitch width was as high as 100ms. Therefore, we expect that the effect of variations in latency time on the validity of the results presented here is minimal. Future experiments should assess this by measuring conduction velocity and latency time

Since typically stimulations by the electrical technique were done first followed by the electrochemical technique, it might be argued that the effect on motor unit recruitment is caused by the fatigue of fast twitch motor units. The stimulations were performed at a low frequency (1Hz) for short periods of time, however, which is not expected to lead to fatigue.

Motor unit recruitment order is critical due to its implications on muscle fatigue. The ultimate measure of the effectiveness of this novel stimulation technique is whether it can afford patients decreased fatigue with Functional Electrical Stimulation. Therefore, future experiment should compare muscle fatigue using traditional electrical stimulation and using this novel electrochemical stimulation.

5. Conclusions

Calcium depletion through ion-selective electrodes had previously been shown to decrease threshold current *in vitro* for direct nerve stimulation, with potential applications in Functional Electrical Stimulation. In this work, flexible polyimide-based cuff electrodes were fabricated by micro-fabrication techniques to enable future implantation and testing *in vivo*. The devices developed are flexible, elastic, and conductive and exhibit strong metal-polyimide adhesion. The devices were used for direct nerve stimulation *in vitro*; it was found that ion-selective membranes can effectively decrease the stimulation threshold current compared to bare electrodes. Furthermore, it was found that the ion-selective electrode is more effective at modulating nerve stimulation when it contours the nerve than when it contacts it at one point (planar electrode). Additionally, the effect of ion-selective membranes on recruitment of motor units was assessed. It was found that ion-selective electrodes are more effective at recruiting slow twitch motor units, particularly at low force outputs. This has great implications on motor unit recruitment order, which is currently one of the primary obstacles for clinical applications of Functional Electrical Stimulation. This technology shows promise for the development of safe, low-power neuro-prosthetics that exhibit physiological motor unit recruitment order.

6. Appendix – Mask Design

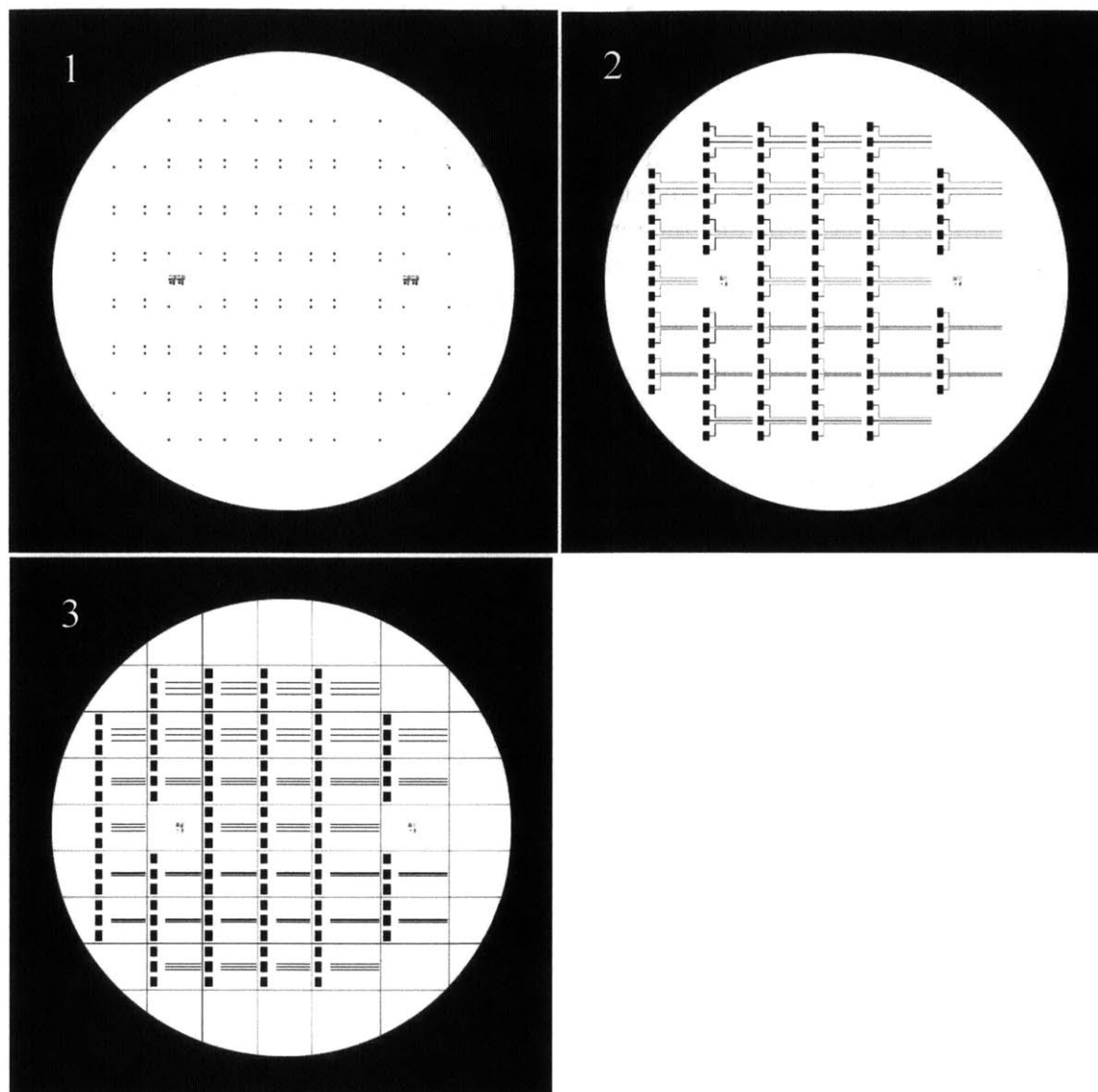


Figure 21: Photolithography Masks Design. The first mask is used to pattern the first layer of photodefinable polyimide (HD 4110). The second mask is used to pattern the image reversal photoresist (AZ 5214E). The third mask is used to pattern the second layer of photodefinable polyimide.

The first mask is used to create the holes (locking mechanism) in the underlying polyimide. The polyimide used is photodefinable as a negative photoresist, therefore, exposed areas become insoluble to the developer. The second mask is used to pattern the image reversal photoresist which is used as part of the metallization process through liftoff. The exposed areas are insoluble to the developer. The third mask is used to pattern the second layer of polyimide so as to expose the electrodes at the nerve sites and the wire contact pads, but insulate the rest of the device.

Bibliography

1. HENNEMAN E, SOMJEN G, CARPENTER DO. Functional significance of cell size in spinal motoneurons. *J Neurophysiol.* 1965;28:560-580.
2. HENNEMAN E. Relation between size of neurons and their susceptibility to discharge. *Science.* 1957;126(3287):1345-1347.
3. MCPHEDRAN AM, WUERKER RB, HENNEMAN E. Properties of motor units in a heterogeneous pale muscle (M. gastrocnemius) of the cat. *J Neurophysiol.* 1965;28:85-99.
4. Song YA, Melik R, Rabie AN, et al. Electrochemical activation and inhibition of neuromuscular systems through modulation of ion concentrations with ion-selective membranes. *Nat Mater.* 2011;10(12):980-986.
5. Alojz R. Kralj, Tadej Bajd. *Functional electrical stimulation: Standing and walking after spinal cord injury.* CRC Press; 1989.
6. Peckham PH, Knutson JS. Functional electrical stimulation for neuromuscular applications. *Annu Rev Biomed Eng.* 2005;7:327-360.
7. Gater DR, Jr, Dolbow D, Tsui B, Gorgey AS. Functional electrical stimulation therapies after spinal cord injury. *NeuroRehabilitation.* 2011;28(3):231-248.
8. Ward AR, Shkuratova N. Russian electrical stimulation: The early experiments. *Phys Ther.* 2002;82(10):1019-1030.
9. Peckham PH, Keith MW, Kilgore KL, et al. Efficacy of an implanted neuroprosthesis for restoring hand grasp in tetraplegia: A multicenter study. *Arch Phys Med Rehabil.* 2001;82(10):1380-1388.
10. Kilgore KL, Hoyen HA, Bryden AM, Hart RL, Keith MW, Peckham PH. An implanted upper-extremity neuroprosthesis using myoelectric control. *J Hand Surg Am.* 2008;33(4):539-550.
11. Smith B, Peckham PH, Keith MW, Roscoe DD. An externally powered, multichannel, implantable stimulator for versatile control of paralyzed muscle. *IEEE Trans Biomed Eng.* 1987;34(7):499-508.
12. Keith MW, Peckham PH, Thrope GB, et al. Implantable functional neuromuscular stimulation in the tetraplegic hand. *J Hand Surg Am.* 1989;14(3):524-530.
13. Ottobock - ActiGait. http://www.ottobock.com/cps/rde/xchg/ob_com_en/hs.xsl/4762.html. Updated 2012. Accessed 09/07, 2012.

14. Burridge JH, Haugland M, Larsen B, et al. Phase II trial to evaluate the ActiGait implanted drop-foot stimulator in established hemiplegia. *J Rehabil Med*. 2007;39(3):212-218.
15. Rushton DN, Donaldson ND, Barr FM, et al. Lumbar root stimulation for restoring leg function: Results in paraplegia. *Artif Organs*. 1997;21(3):180-182.
16. Davis R, Patrick J, Barriskill A. Development of functional electrical stimulators utilizing cochlear implant technology. *Med Eng Phys*. 2001;23(1):61-68.
17. Kobetic R, Triolo RJ, Uhler JP, et al. Implanted functional electrical stimulation system for mobility in paraplegia: A follow-up case report. *IEEE Trans Rehabil Eng*. 1999;7(4):390-398.
18. Rushton DN. Functional electrical stimulation. *Physiol Meas*. 1997;18(4):241-275.
19. Tyler DJ, Durand DM. A slowly penetrating interfascicular nerve electrode for selective activation of peripheral nerves. *IEEE Trans Rehabil Eng*. 1997;5(1):51-61.
20. Fang ZP, Mortimer JT. A method to effect physiological recruitment order in electrically activated muscle. *IEEE Trans Biomed Eng*. 1991;38(2):175-179.
21. Tai C, Jiang D. Selective stimulation of smaller fibers in a compound nerve trunk with single cathode by rectangular current pulses. *IEEE Trans Biomed Eng*. 1994;41(3):286-291.
22. Hennings K, Kamavuako EN, Farina D. The recruitment order of electrically activated motor neurons investigated with a novel collision technique. *Clin Neurophysiol*. 2007;118(2):283-291.
23. Petrofsky JS. Control of the recruitment and firing frequencies of motor units in electrically stimulated muscles in the cat. *Med Biol Eng Comput*. 1978;16(3):302-308.
24. Hurlbert RJ, Tator CH, Theriault E. Dose-response study of the pathological effects of chronically applied direct current stimulation on the normal rat spinal cord. *J Neurosurg*. 1993;79(6):905-916.
25. Petruska JC, Hubscher CH, Johnson RD. Anodally focused polarization of peripheral nerve allows discrimination of myelinated and unmyelinated fiber input to brainstem nuclei. *Exp Brain Res*. 1998;121(4):379-390.
26. Kilgore KL, Bhadra N. Nerve conduction block utilising high-frequency alternating current. *Med Biol Eng Comput*. 2004;42(3):394-406.
27. Grill WM, Mortimer JT. Stimulus waveforms for selective neural stimulation. *Engineering in Medicine and Biology Magazine, IEEE*. ;14(4):375.
28. Solomonow M. External control of the neuromuscular system. *IEEE Trans Biomed Eng*. 1984;31(12):752-763.

29. Swallow M. Fibre size and content of the anterior tibial nerve of the foot. *J Neurol Neurosurg Psychiatry*. 1966;29(3):205-213.
30. Thomas CK, Nelson G, Than L, Zijdwind I. Motor unit activation order during electrically evoked contractions of paralyzed or partially paralyzed muscles. *Muscle Nerve*. 2002;25(6):797-804.
31. Butson CR, Miller IO, Normann RA, Clark GA. Selective neural activation in a histologically derived model of peripheral nerve. *J Neural Eng*. 2011;8(3):036009.
32. Tyler DJ, Durand DM. Functionally selective peripheral nerve stimulation with a flat interface nerve electrode. *IEEE Trans Neural Syst Rehabil Eng*. 2002;10(4):294-303.
33. Tarler MD, Mortimer JT. Selective and independent activation of four motor fascicles using a four contact nerve-cuff electrode. *IEEE Trans Neural Syst Rehabil Eng*. 2004;12(2):251-257.
34. Merrill DR, Bikson M, Jefferys JG. Electrical stimulation of excitable tissue: Design of efficacious and safe protocols. *J Neurosci Methods*. 2005;141(2):171-198.
35. Rodriguez FJ, Ceballos D, Schuttler M, et al. Polyimide cuff electrodes for peripheral nerve stimulation. *J Neurosci Methods*. 2000;98(2):105-118.
36. Fibre-selective recording from peripheral nerves using a multiple-contact cuff: Report on pilot pig experiments. *EMBC: Proc.Int.Annu.Conf.of IEEE Engineering in Medicine and Biology Society*. 2011:3103.
37. Stieglitz T, Schuettler M, Rubehn B, Boretius T, Badia J, Navarro X. Evaluation of polyimide as substrate material for electrodes to interface the peripheral nervous system. *Neural Engineering (NER), 2011 5th International IEEE/EMBS Conference on*. 2011:529-533.
38. Viventi J, Kim DH, Vigeland L, et al. Flexible, foldable, actively multiplexed, high-density electrode array for mapping brain activity in vivo. *Nat Neurosci*. 2011;14(12):1599-1605.
39. Bakker E, Bühlmann P, Pretsch E. Polymer membrane ion-selective electrodes? what are the limits? *Electroanalysis*. 1999;11(13):915-933.
40. Ammann D, Buehrer T, Schefer U, Mueller M, Simon W. Intracellular neutral carrier-based Ca^{2+} microelectrode with subnanomolar detection limit. *Pfluegers Archiv*. 1987;409(3):223-228.
41. BRINK F. The role of calcium ions in neural processes. *Pharmacol Rev*. 1954;6(3):243-298.
42. Bergkessel N, Bergstresser T, Chiang S, Russell D. Adhesion performance of polyimide adhesiveless flexible laminates having nickel based tiecoats. . 1997.
43. Wieler M, Stein RB, Ladouceur M, et al. Multicenter evaluation of electrical stimulation systems for walking. *Arch Phys Med Rehabil*. 1999;80(5):495-500.

44. Rousche PJ, Pellinen DS, Pivin DP, Jr., Williams JC, Vetter RJ, kirke DR. Flexible polyimide-based intracortical electrode arrays with bioactive capability. *Biomedical Engineering, IEEE Transactions on*. 2001;48(3):361-371.
45. Llewellyn ME, Thompson KR, Deisseroth K, Delp SL. Orderly recruitment of motor units under optical control in vivo. *Nat Med*. 2010;16(10):1161-1165.